BBA - Biomembranes 1866 (2024) 184256

Contents lists available at ScienceDirect

BBA - Biomembranes

journal homepage: www.elsevier.com/locate/bbamem

Spontaneous transfer of small peripheral peptides between supported lipid bilayer and giant unilamellar vesicles

Emanuela Efodili [a], Ashlynn Knight [b], Maryem Mirza [c], Cedric Briones [a], Il-Hyung Lee [a,*]

[a] Department of Chemistry and Biochemistry, Montclair State University, Montclair, NJ 07043, USA
[b] Department of Biology, Montclair State University, Montclair, NJ 07043, USA
[c] College of humanities and social sciences, Montclair State University, Montclair, NJ 07043, USA

ARTICLE INFO

Keywords:
Membrane fusion
Vesicular trafficking
Lipid membrane
Fluorescence imaging
Membrane reconstitution
Supported lipid bilayer
Giant unilamellar vesicle

ABSTRACT

Vesicular trafficking facilitates material transport between membrane-bound organelles. Membrane protein cargos are trafficked for relocation, recycling, and degradation during various physiological processes. *In vitro* fusion studies utilized synthetic lipid membranes to study the molecular mechanisms of vesicular trafficking and to develop synthetic materials mimicking the biological membrane trafficking. Various fusogenic conditions which can induce vesicular fusion have been used to establish synthetic systems that can mimic biological systems. Despite these efforts, the mechanisms underlying vesicular trafficking of membrane proteins remain limited and robust *in vitro* methods that can construct synthetic trafficking systems for membrane proteins between large membranes (>1 μm^2) are unavailable. Here, we provide data to show the spontaneous transfer of small membrane-bound peptides (~4 kD) between a supported lipid bilayer (SLB) and giant unilamellar vesicles (GUVs). We found that the contact between the SLB and GUVs led to the occasional but notable transfer of membrane-bound peptides in a physiological saline buffer condition (pH 7.4, 150 mM NaCl). Quantitative and dynamic time-lapse analyses suggested that the observed exchange occurred through the formation of hemi-fusion stalks between the SLB and GUVs. Larger protein cargos with a size of ~77 kD could not be transferred between the SLB and GUVs, suggesting that the larger-sized cargos limited diffusion across the hemi-fusion stalk, which was predicted to have a highly curved structure. Compositional study showed Ni-chelated lipid head group was the essential component catalyzing the process. Our system serves as an example synthetic platform that enables the investigation of small-peptide trafficking between synthetic membranes and reveals hemi-fused lipid bridge formation as a mechanism of peptide transfer.

1. Introduction

Vesicular trafficking is a process of material transport between two lipid bilayers. In living cells, this occurs between different membrane-bound organelles such as plasma membranes, lysosomes, and endoplasmic reticulum [1–3]. The process often involves vesicular fusion which is an event where two lipid bilayers contact, hemi-fuse, and completely fuse to become a continuous bilayer [4,5]. Vesicular trafficking is one of the most fundamental activities in living cells, thus malfunction of the trafficking is known to cause various diseases [6,7]. Naturally, understanding the molecular mechanism of vesicular trafficking has been an intense area of research. Vesicular trafficking by synthetic lipid vesicle systems has been used widely to study the molecular mechanism of the trafficking process in controlled environments [8–10] and also to find applications as biomimetic materials in creation of artificial life [11,12] and drug delivery systems [13,14]. Structural and biophysical studies on trafficking systems made significant progress in understanding the molecular mechanism in the last few decades, but we currently still do not have enough understanding and techniques to synthetically reproduce and construct a system capable of performing vesicular trafficking of membrane proteins.

Physiological trafficking may involve several tens of proteins, and each trafficking pathway between different organelles involve unique set of proteins, thus making study of molecular mechanism challenging [1,15]. Cellular imaging by fluorescence microscopy is often performed to study the localization of different proteins at the sites of trafficking [16–18] and hypothetical mechanism can be tested with purified proteins *in vitro* by reconstitution study [8,10,19]. Such studies often focus

* Corresponding author.
E-mail address: leei@montclair.edu (I.-H. Lee).

https://doi.org/10.1016/j.bbamem.2023.184256
Received 7 June 2023; Received in revised form 8 October 2023; Accepted 14 November 2023
Available online 20 November 2023
0005-2736/Published by Elsevier B.V.

on the structure-function relationship of the proteins with known hypothetical roles in the process. The studies are crucial for potential drug development targeting the trafficking processes, but physiological trafficking process tends to be very complex, so establishing a simple physical model toward the development of simple synthetic system is not trivial from such studies.

In vitro studies to develop synthetic fusion system has been hinting on minimal necessary components for successful vesicular fusion. Such studies often use chemical methods that might not even be physiologically relevant looking for applications of vesicular trafficking as biomimetic materials. Various fusogenic conditions are known to catalyze the fusion or formation of hemi-fusion stalks between lipid bilayers. Example fusogenic conditions include multivalent cations [20,21], freeze-thawing [22,23], nano-particle interaction [24,25], and functional peptide mediated fusions [26,27] to name a few. Previous reports show examples of vesicular content inside may be transferred to another vesicle by fusion [28,29]. However, examples on membrane proteins, proteins spanning or peripherally anchored to the lipid membranes, being transferred [26,30] have been underexplored, limiting our understanding on membrane protein trafficking processes.

In this study, we report a case of synthetic vesicular trafficking of peripheral peptides between supported lipid bilayer (SLB, a lipid bilayer formed on glass surface), and giant unilamellar vesicles (GUV, single layered lipid vesicle with diameter >1 μm). We used confocal laser scanning microscopy (CLSM) and wide field fluorescence microscopy to monitor the exchange of small peptides anchored on the lipid membranes from SLB to GUV. Our results show that such transfer may occur spontaneously between SLB and GUV under the neutral saline condition of pH 7.4 and 150 mM NaCl by hemi-fusion stalk formation between SLB and GUV.

2. Methods

2.1. GUV preparation

The GUVs were prepared by gentle hydration [31–33]. This involved combining a lipid mixture of calculated composition in a clean round-bottomed flask using glass syringes (Hamilton Company). The composition of the GUV used in this study was 30 % 1,2-dioleoyl-sn-glycero-3-phosphoethanolamine (DOPE), 5 % 1,2-dioleoyl-sn-glycero-3-phospho-L-serine (DOPS), 65 % 1,2-dioleoyl-sn-glycero-3-phosphocholine (DOPC) by mol% unless specified otherwise. DOPC is a commonly used model lipid for its low melting temperature and fluidity, DOPS is a net negatively charged lipid at pH 7.4 introduced to facilitate vesicle swelling process, DOPE is a lipid that can facilitate flexible deformation of the lipid membranes by curved structure formation without affecting the membrane fluidity [34]. Negative control sample composition was 5 % Ni-DGS, 95 % DOPC. 0.1 % of the DiD (Invitrogen) replaced the DOPC for fluorescence for the experiments shown in Figs. 1–2, 4–5 and no fluorescent reporter was used for experiments in Figs. 3, 6–7. The mixture was then dried to a thin film with nitrogen gas, to evaporate the chloroform solvent, while on a hot plate set to maintain the temperature at 55–60 °C. The flask was placed in a room-temperature vacuum chamber for the sample to dry further for at least 1 h. 1 mL of 320 mM sucrose solution was introduced into the flask, the flask was sealed, and incubated overnight at 37 °C to induce vesicle swelling by hydration. Following incubation, the now GUVs were centrifuged for 5 min at 12,000*g* to remove large lipid aggregates. 600–800 μL of aggregate free

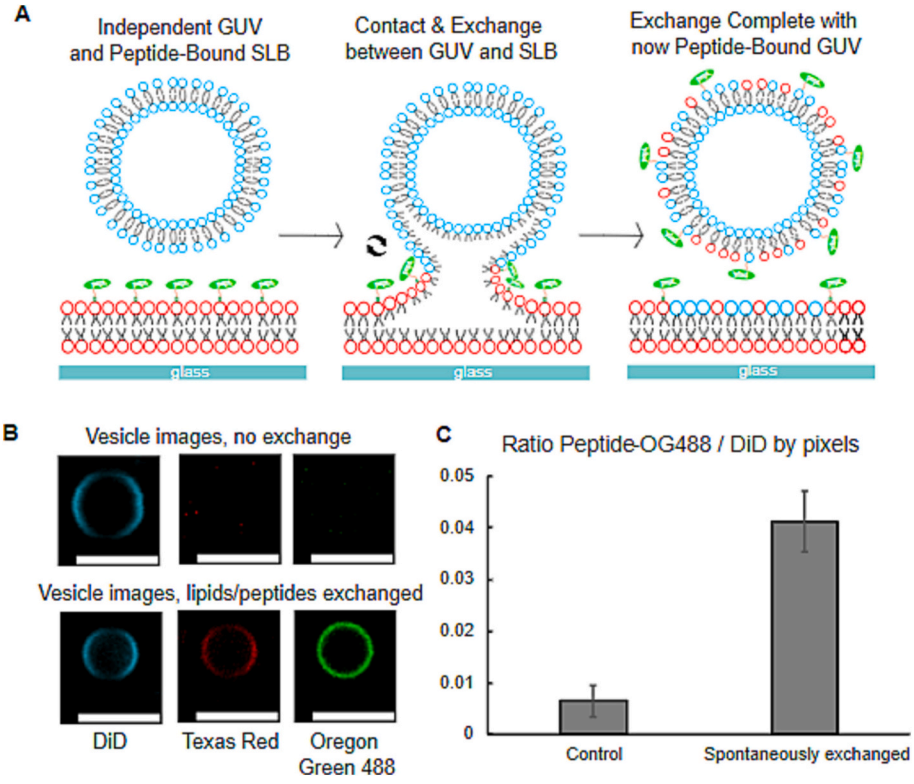

Fig. 1. Phospholipid membrane fusion and protein transfer from SLB to GUV. (A) Schematic of the SLB to GUV exchange with peptide anchored onto the SLB. The lipid composition for the GUV was 64.9 % DOPC, 30 % DOPE, 5 % DOPS, and 0.1 % DiD. The lipid composition for the SLB was 64.9 % DOPC, 30 % DOPE, 5 % Ni-DGS, and 0.1 % TR-DHPE. (B) Example images of DiD, TR-DHPE, and peptide-OG488 fluorescent vesicles when the exchange does and does not occur. Scale bars are set to 5 μm. (C) Statistical distribution by pixels of the ratio of LAT-OG488 to DiD in a negative control setting compared to spontaneous exchange, where spontaneous exchange occurs at an observable rate. Negative control sample was just vesicles alone with the composition of 5 % Ni-DGS, 94.9 % DOPC, and 0.1 % DiD. Therefore, the basal ratio of the control sample represents optical crosstalk and background level detection by the analysis. Error bars represent standard errors of $N = 22$ images from three independently prepared lipid bilayers.

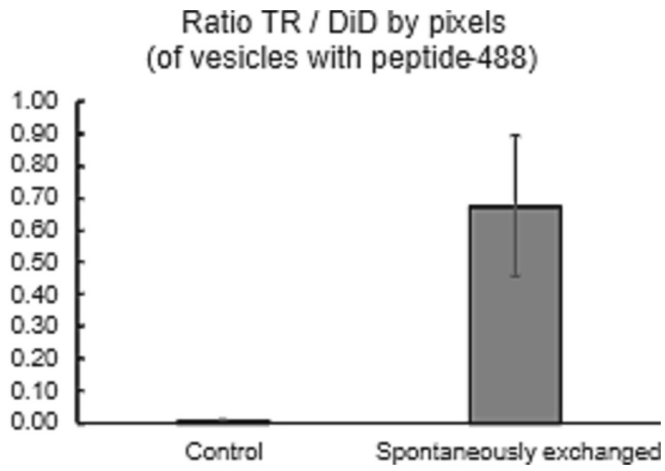

Fig. 2. Statistical distribution by pixels of the ratio of TR-DHPE vesicles with LAT-OG488 to DiD vesicles with LAT-OG488. There is an observable increase in TR-DHPE to DiD vesicles that spontaneously exchanged peptides. Error bars represent standard errors of $N = 22$ images from three independently prepared lipid bilayers.

solution were collected and stored at 4 °C until use. The lipids used were obtained from Avanti Polar Lipids Inc. as. High purity laboratory water that was properly purified and deionized was used for the experiments.

2.2. SLB preparation and functionalization

The small unilamellar vesicles (SUVs) were prepared by extrusion [8]. This involved combining a lipid mixture of calculated composition in a clean round-bottomed flask using glass pipettes (Hamilton). The composition of the SUV used in this study was 30 % DOPE, 5 % Ni bound 1,2-dioleoyl-sn-glycero-3-[(N-(5-amino-1-carboxypentyl)iminodiacetic acid)succinyl] (Ni-DGS), 65 % DOPC unless specified otherwise. 0.1 % of the Texas Red 1,2-Dihexadecanoyl-sn-Glycero-3-Phosphoethanolamine (TR-DHPE, Invitrogen) replaced the DOPC for the experiments in Figs. 1–2, 4–5; 0.1 % DiD for the experiments in Fig. 3; and 0.1 % OG488-DHPE (Invitrogen) replaced the DOPC for the experiments in Figs. 6–7. Ni-DGS serves the role of anchoring peptides and proteins to the membranes by poly histidine-Ni chelation. The mixture was proceeded to dry with nitrogen gas, to evaporate the chloroform solvent, while on a hot plate set to 55–60 °C, to ensure temperature control. The flask was placed in a room-temperature vacuum chamber for the sample to dry further at least for 1 h. 1 mL of deionized water was introduced into the flask, covered, then freeze-thawed at least three times using Lab Armor metal beads (Gibco) stored at −80 °C. SUV extrusion was performed using handheld mini extruder nine times using a 100 nm pore-size polycarbonate filter (Whatman). Final SUVs were stored at 4 °C until use. The lipids and handheld mini extruder were obtained from Avanti Polar Lipids Inc.

The SLB was prepared by SUV rupturing. Assembled was an Attofluor chamber (Invitrogen) with a round cover glass (25CIR-1, ThermoFisher), that was sonicated for 30 min in solution of isopropyl alcohol: water = 1:1 by volume, then etched with acid piranha solution (30 % hydrogen peroxide:concentrated sulfuric acid = 1:3 by volume). A silicon O-ring was placed for a reduced sample space. 100 μL of SUV solution and 100 μL of phosphate buffer including magnesium chloride (20 mM phosphate, 5 mM $MgCl_2$, pH 7.4) were combined in an Eppendorf tube. 200 μL of the mixture was dispensed into the chamber and left to incubate for 30 min at room temperature. The SUVs spontaneously ruptured on the piranha-etched glass to generate the SLB [35]. Without exposing the SLB to the air to avoid oxidation of the bilayer, the chamber was rinsed ten times with Hepes buffer (20 mM Hepes, 150 mM NaCl, pH 7.4). When incubating the peptide or protein on the SLB surface, a diluted amount of the peptide/protein concentration (10 nM – 1 μM) was introduced into the chamber and left to sit for 30 min. Linker for activation of T-cell (LAT) peptide [33] and Small Ubiquitin-like modifier 3–Green fluorescence protein (SUMO3-GFP) [31,36] included his-tags to covalently bind to the Ni of the Ni-DGS lipids. LAT peptide was covalently labeled (Cysteine-maleimide chemistry) with Oregon Green 488 (OG488, Invitrogen) or Alexa Fluor 647 (A647, Invitrogen), and SUMO3-GFP is inherently fluorescent by the GFP fluorescence. Without exposing the SLB to the air, the chamber was then rinsed ten times with Hepes buffer (20 mM Hepes, 150 mM NaCl, pH 7.4). To ensure stable protein binding, incubation proceeded for another 20 min [37], then finally rinsed 7× without exposing the SLB to the air. Fluorescence bleaching after photobleaching (FRAP) measurement was performed to ensure fluidity of the SLB formed (Supplementary S1) [8]. For the adhesion control experiment, 300 mM Glucose with 20 mM Hepes (pH 7.0) was used instead of the saline buffer.

2.3. Imaging sample preparation

After checking the creation of fluidic SLB, depending on the experiment and composition, 1–10 μL of GUV solution was added to the chamber with Hepes buffer to ensure an adequate amount of vesicles were observable per image, then settled for 5 min on the microscope stage. This step was where spontaneous interaction between the SLB-peptide (protein) and GUV was observed. Time-lapse movies and z-stack images with multi-color excitation were taken accordingly to observe exchange of lipids and peptides (proteins). At least 30 min of interaction between SLB and GUVs was allowed at room temperature (22 °C) before taking the final z-stack images. For the cationic shock experiment, after the initial incubation was complete, an equal volume of 2 mM $LaCl_3$ solution in Hepes buffer was gently added to introduce 1 mM La^{3+} concentration final. The $LaCl_3$ triggered the facilitated lipid exchange between the SLB and GUV. For the calcium experiments, final concentration was set to be 10 mM Ca^{2+}. (by $CaCl_2$) Time-lapse movies and z-stack images were taken accordingly. At least 30 min of interaction was allowed before taking the final z-stack images. The sample samples was covered with Petri dish at all times during imaging to prevent sample evaporation.

For the negative control sample, which was to calculate the noise level of co-localization, sample chamber was assembled the same way without doing the piranha etching of the cover glasses. 5 mg/mL BSA (Sigma-Aldrich) solution was used to block the surface for 30 min, followed by addition of GUV solution for image acquisition using the same conditions as the imaging of other samples.

2.4. Fluorescence imaging conditions

2.4.1. Confocal laser scanning microscopy imaging

Images shown in Figs. 1–2, 4–5 were collected using CLSM. Briefly, a Nikon Ti-E-based C2 confocal microscope was used (Nikon, Japan). Excitation laser lights of 488, 561, and 640 nm were used with matching emission filters to collect signals from the fluorescent molecules. A Nikon Plan Apo 100 × NA 1.45 oil immersion objective was used without further magnifying the lens in the optical path. The typical mode of scanning was to collect data as 1024 × 1024 pixels spanning a 127.3 μm × 127.3 μm area, whereas motorized z-axis movement allowed the automated acquisition of z-stack images. All the example images shown were originally collected by taking a z-stack every 1 μm apart which is typically a great sampling in the z-direction considering the resolution of confocal laser scanning and the size of the GUVs. Most representative image sections showing clear contour of the vesicle fluorescence were chosen for further analysis typically images ~3–5 μm above the bottom.

2.4.2. Wide field fluorescence microscopy imaging

A Nikon Ti2E-based inverted epifluorescence microscope system

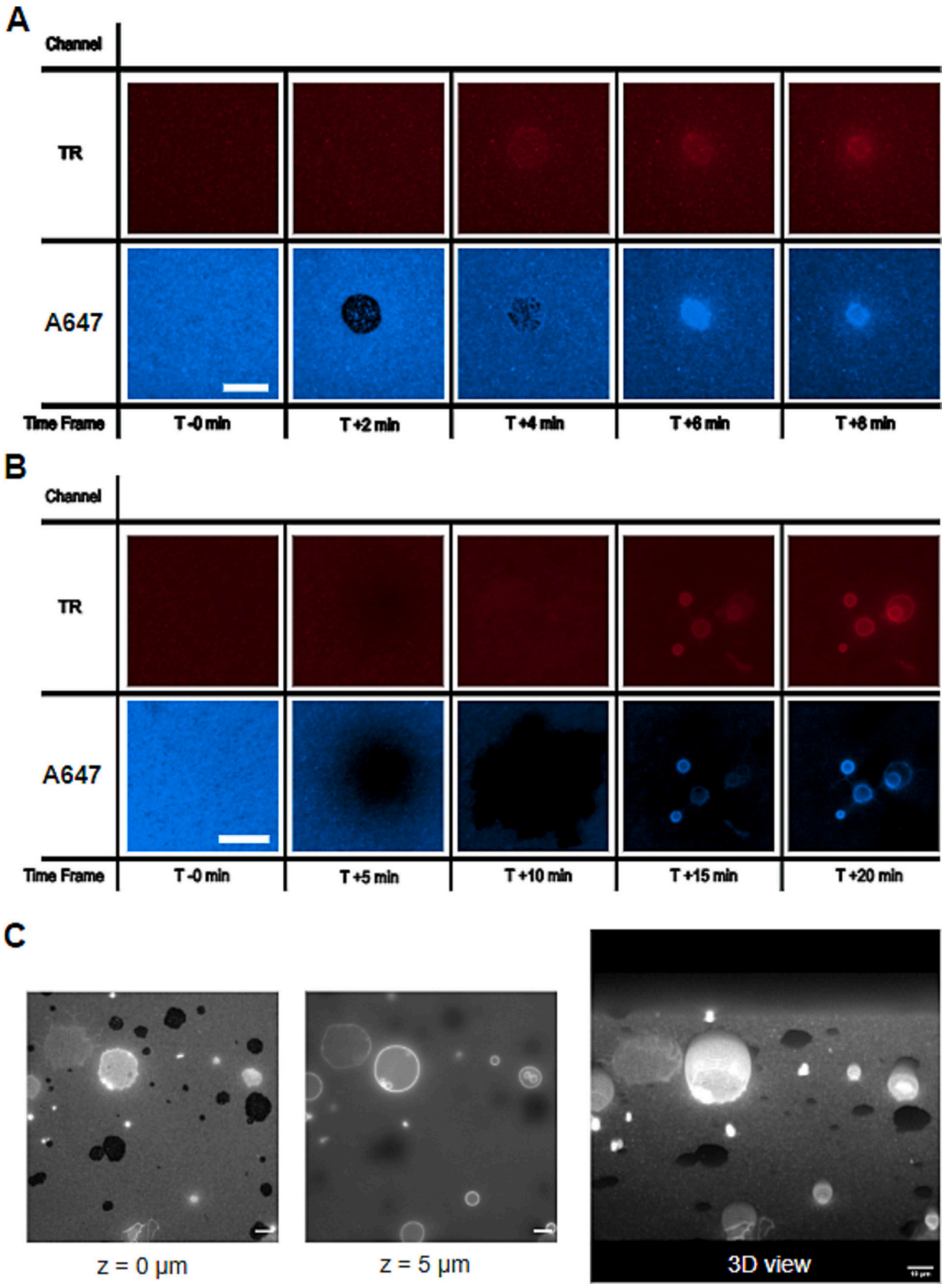

Fig. 3. Time lapse movies by wide field fluorescence imaging and 3-dimensional view image of vesicles visible from contact and peptide exchange on the SLB. (A) Colorless GUVs touch and exchange with the SLB and peptide-A647 incubated on the SLB. Interaction is observed right on the surface and time-lapse images of 0, +2, +4, +6, +8 min are shown. The SLB is viewed in the Texas Red channel distinguished in red. Peptide-A647 is viewed in the Cy5 channel distinguished in blue. (B) Colorless GUVs touch and exchange with the SLB and peptide-A647 incubated on the SLB. Interaction is observed right on the surface and defined vesicles are seen. Time-lapse images of 0, +5, +10, +15 + 20 min are shown. The SLB is viewed in the Texas Red channel distinguished in red. Peptide-A647 is viewed in the Cy5 channel distinguished in blue. Scale bars are set to 5 µm. (C) Images taken on the SLB surface and 5 µm above the surface to display the interaction and exchange that took place between GUVs and the SLB. 21 sections of z-stack images for every 1 µm were used to reconstruct the 3D view. Dark contact sites and peptide exchanged vesicles are clearly visible by peptide-A647 fluorescence. Scale bars are 10 µm. Kinetic trace analysis can be found in Supplementary S4.

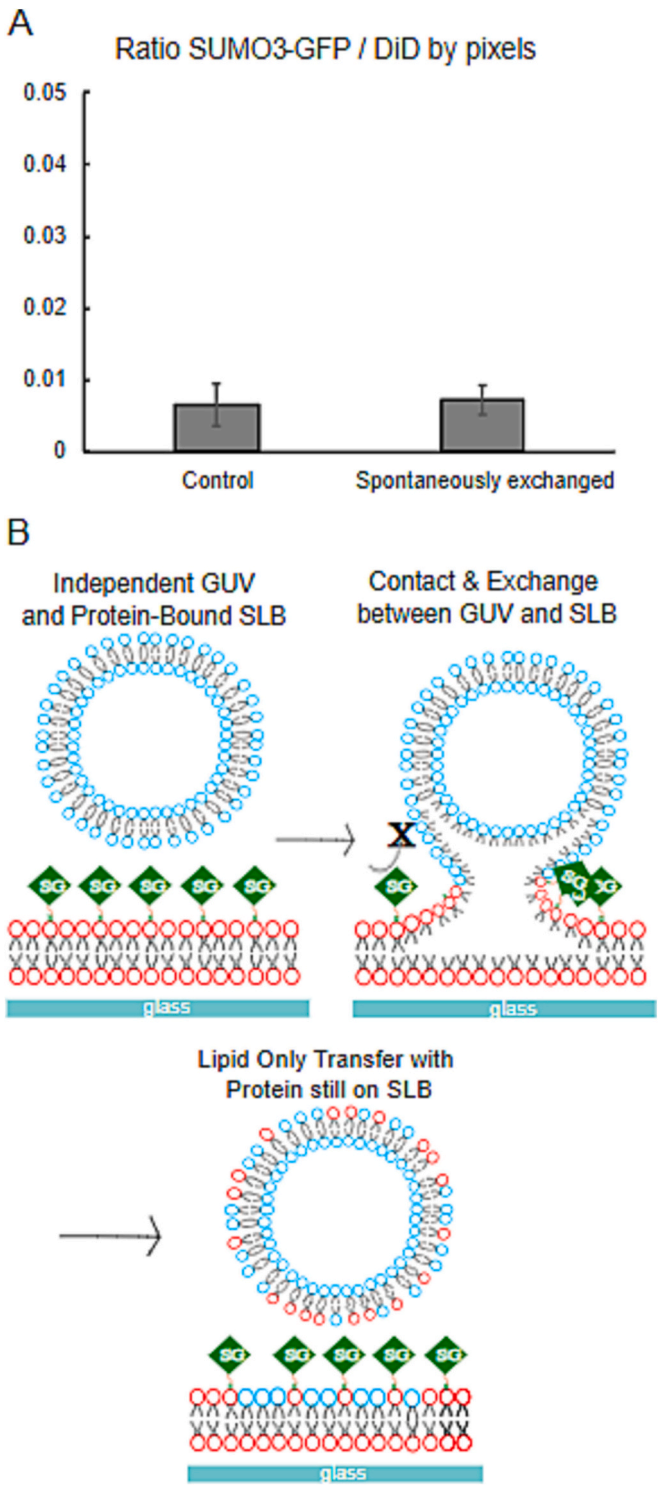

Fig. 4. SUMO3-GFP exchange experiments. (A) Statistical distribution by pixels of the ratio of SUMO3-GFP to DiD in a negative control setting compared to spontaneous exchange. There is no significant difference between the control and the spontaneous exchange samples. (B) Schematic of the SLB to GUV exchange with SUMO3-GFP anchored onto the SLB. Bulky SUMO3-GFP proteins (76kD) fail to make transfer from SLB to GUV. The lipid composition for the GUV was 64.9 % DOPC, 30 % DOPE, 5 % DOPS, and 0.1 % DiD. The lipid composition for the SLB was 64.9 % DOPC, 30 % DOPE, 5 % Ni-DGS, and 0.1 % TR-DHPE. Error bars represent standard errors of $N = 21$ images from three independently prepared lipid bilayers.

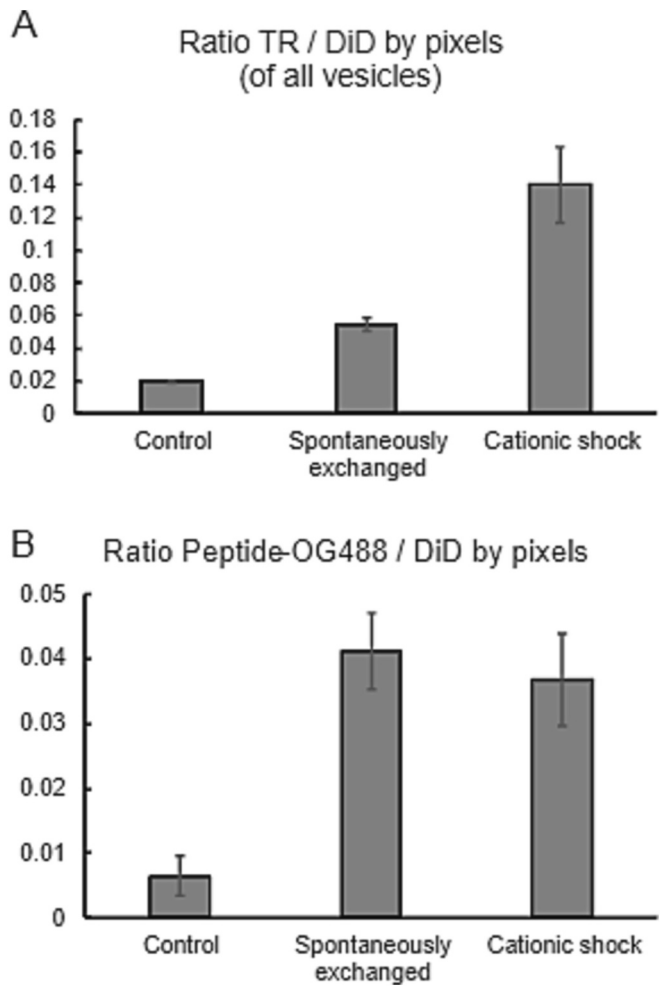

Fig. 5. Cationic shock experiments to catalyze lipids exchange. (A) Statistical distribution by pixels of the ratio of TR-DHPE vesicles to DiD vesicles in a negative control setting compared to spontaneous exchange and cationic shock with lanthanide. Cationic shock with La^{3+} has the greatest effect on the interaction, increasing the proportion of TR-DHPE vesicles to DiD vesicles facilitating the lipid exchange. (A) Statistical distribution by pixels of the ratio of LAT-OG488 to DiD in a negative control setting compared to spontaneous exchange and cationic shock with La^{3+}. While cationic shock does catalyze the lipid exchange, it does not result in further exchange of peptides between SLB and GUVs.

(Nikon, Japan) was used for FRAP and time-lapse imaging and DIC-coupled imaging shown in Figs. 3, 6–7. A light-emitting diode (LED) white light excitation source (Lumencor) was optically filtered with multiple optical filters and dichroic mirrors to excite and collect fluorescence emission optimized for Cy5, GFP, and Texas Red, respectively. The Nikon Apo 100× TIRF oil objective with a numerical aperture of 1.49 was used for imaging. Single-molecule sensitivity with a high quantum yields scientific complementary metal–oxide–semiconductor camera was used for data collection (Hamamatsu ORCA Flash 4.0, Hamamatsu, Japan). Automatic z-position control was used for precise z-stack acquisition and x, and y positions were controlled manually. Time lapse images were taken by choosing a z-section(s) of interest to repeat image acquisition at set time intervals (15 s–60 s). Due to faster acquisition time, wide field fluorescence imaging was often advantageous when observation of dynamic change was the goal. Micromanager (https://micro-manager.org/), an ImageJ (https://imagej.nih.gov/ij/) based software was used to manage the devices. All data collection was performed on a vibration isolation table.

Differential interference contrast microscopy (DIC) was performed

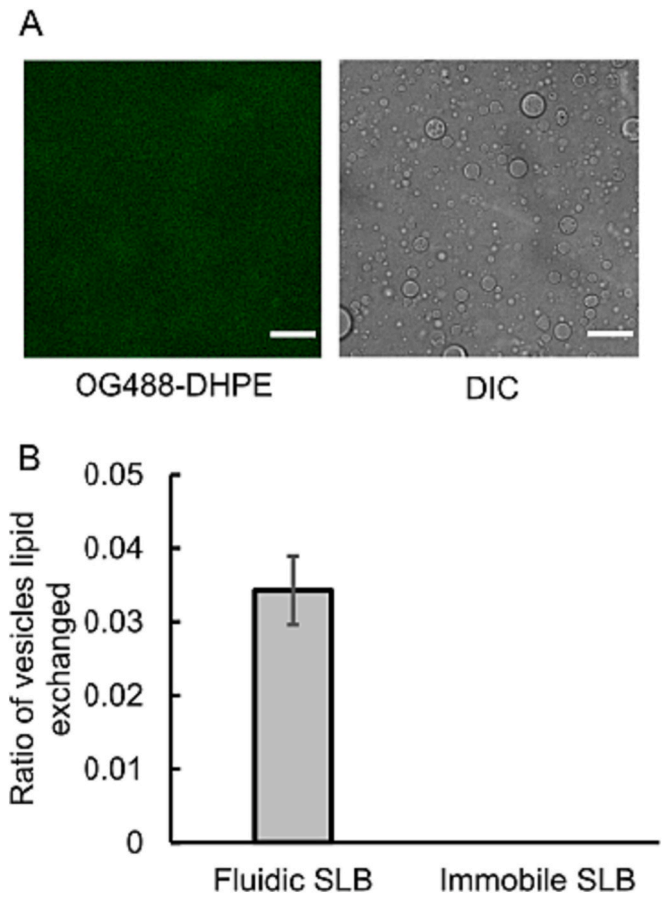

Fig. 6. Immobile SLB does not exchange lipids with GUVs. (A) Representative images of many GUVs after interacting >1 h with immobile SLB (5 % Ni-DGS, 94.9 % DPPC, 0.1 % OG488-DHPE). Images were taken from the wide field fluorescence microscope. Matching images in OG488 fluorescence channel and DIC. Existence of vesicles are obvious from DIC but no fluorescence signal can be found from the GUVs. It indicates that no lipid exchange happened between the SLB and GUVs. Scale bars are 20 μm. (B) Quantitative comparison of the fluidic SLB (5 % Ni-DGS, 30 % DOPE, 64.9 % DOPC, 0.1 % OG488-DHPE) and immobile SLB by counting number of vesicles lipid exchanged. GUVs were fluidic in both cases (5 % DOPS, 30 % DOPE, 64.9 % DOPC, 0.1 % TR-DHPE) Case of immobile SLB exchanging lipids was none basically. ($N = 18$ images from two independently prepared lipid bilayers, error bars represents standard errors).

by illuminating samples with polarized white light which was detected after another emission polarization filter. Such interference imaging can enhance the contrast of objects with typically low optical contrast such as lipid vesicles [38]. We used DIC imaging in some experiments coupled with the wide field fluorescence imaging to estimate number of the vesicles. DIC does not require fluorescence emission thus unambiguously detect all entities regardless of their fluorescence signal.

2.5. Peptide and protein purification

LAT peptide, a derivative from the physiological LAT was synthesized as a service of the company Biomatic and labeled with OG488 and A647 each appropriately following the manufacturer's recommended protocols using Cys-maleimide chemistry [33]. The peptide was chosen as a small model peptide in this study, not particularly due to its specific sequence. The sequence of the LAT peptide was:

HHHHHHHHHHGGSGGSGGD[*pY*]VNVGGSGGSGGD[pY]VNVDKKC

SUMO3-GFP was purified by *E. coli* overexpression following the suggested overexpression condition from the original manuscript that it was developed [36]. A series of chromatography in a fast protein liquid chromatography system (GE Healthcare) was performed [31]. The plasmid was given by the Michael Rosen group (Addgene plasmid #127093).

2.6. Data analysis

For the data presented in this work, we used two different analysis methods suitable for each imaging method used. They are different ways to analyze the data, but eventually quantify the same information, the degree of lipids and peptides exchange. Masking analysis is about 'out of all lipids area visible by fluorescence, what is the ratio of area showing lipid or peptide exchange'? Counting analysis is about 'out of large enough vesicles to be counted as individual entities by DIC, what is the ratio of vesicles showing lipid or peptide exchange?' Figs. 1–5 used masking analysis and Figs. 6–7 used counting analysis.

2.6.1. Masking analysis

Images were analyzed using a home-built automated script. (Run in the freely available software GNU Octave 6.4.1, https://octave.org/, full code available in the Supplementary S8) In the experiments, GUV lipids, SLB lipids, and peripheral peptides (proteins) were labeled by fluorescent dyes with different wavelengths of excitation/emission. We used binary masking and pixel counting to quantify the degree of pixel colocalization between different channels. Colocalized pixels mean overlapping signal at the same location that indicate coexistence of those molecules at the same location. Coexistence within the same lipid membrane thus serves the purpose of quantifying the degree of lipids/peptides exchange. Masking analysis has a merit of removing potential ambiguity of using raw intensity values, which may vary at different optical setups.

One of the z-stack images, typically ones 3–4 μm above the SLB surface was chosen to perform binary masking. Considering the noise level, only pixels representing enough fluorescence signal from lipid membranes were counted. It means pixels with typical level of noise signal was excluded (count as 0) and net signal from the membranes were counted (count as 1). Such analysis was done for all different channels of images and pixels representing the same location in space were compared between different channels. Number of overlapping or colocalizing pixels in multiple channels were counted for quantification. For example, for a certain pixel, if we see high enough signal to be counted in all DiD, TR and OG488 channels, we can call it colocalization in all channels, and that pixel represents a lipid membrane that experienced exchange of both lipids and peptides. If a pixel only has a high enough signal to be counted in DiD channel, we can judge that vesicle membrane existed in that region, but that membrane did not experience lipids or peptides exchange.

For quantification of peptide (protein) transfer, DiD channel (representing lipids originally included in the GUV) were used as a reference channel and OG488 or GFP channel (representing the fluorescence of peptides or proteins) were counted for overlapping pixels to report ratio of [Number of pixels colocalized in OG488 channel] / [Number of pixels representing GUV lipids by DiD]. For lipid exchange analysis, the ratio of [Number of pixels colocalized in TR-DHPE channel representing SLB lipids] / [Number of pixels representing GUV lipids by DiD] was reported. Fig. 2 analysis was done only for pixels with high signal in OG488 (peptide).

2.6.2. Counting analysis

Images were analyzed using a home-built automated script modified from the previous work [39]. Briefly, Circular Hugh transformation algorithm was used to detect circular features that represent GUVs in DIC image 2–4 μm above the SLB surface. For the matching fluorescence channel images, number of vesicles bearing OG488 lipid signal (reporter originally in SLB lipids) and Alexa647 peptides signal (reporter originally in SLB bound peptides) each were counted. Since the GUVs were originally colorless in fluorescence channels, emerging fluorescence

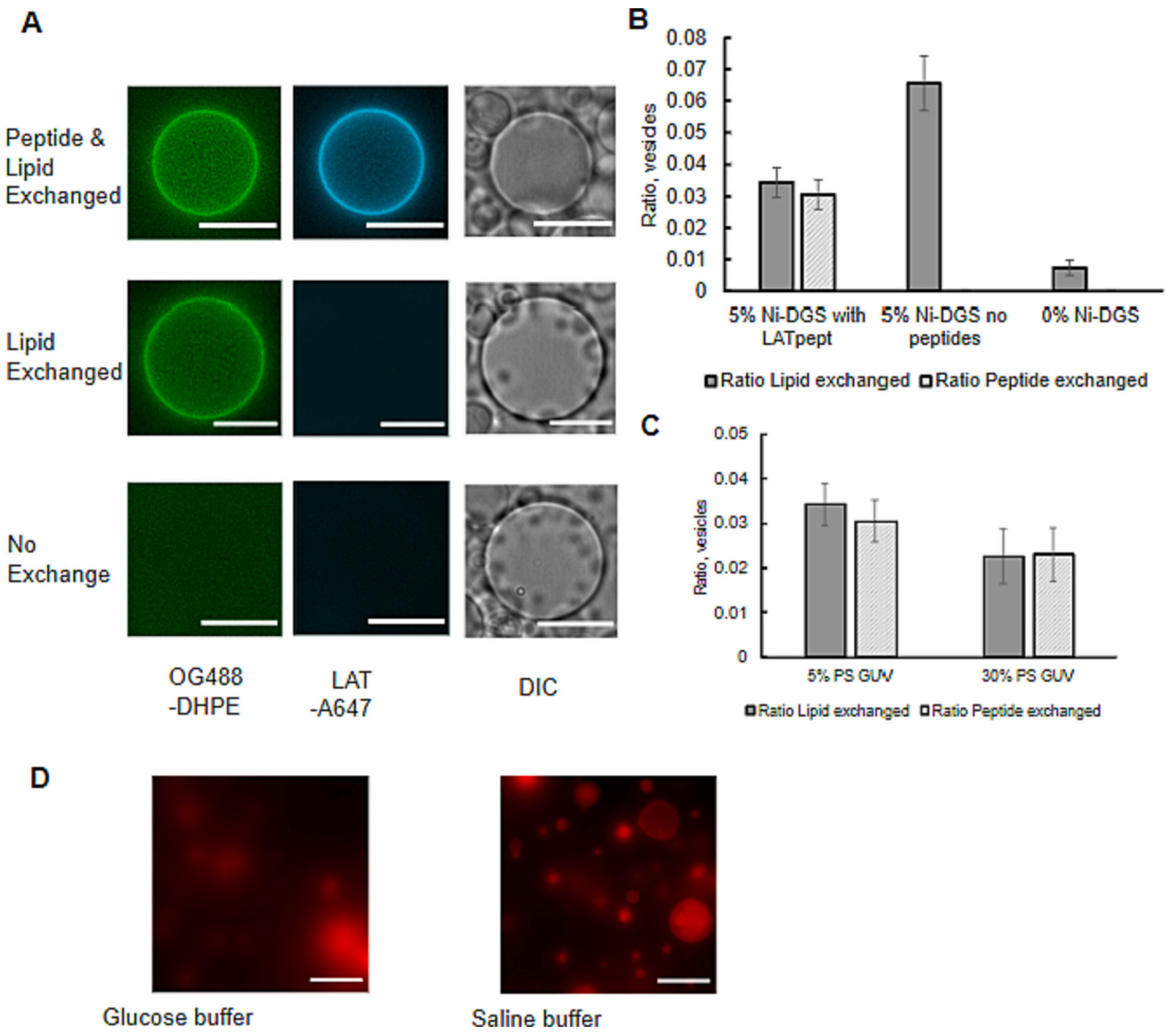

Fig. 7. Lipid composition dependent peptide exchange experiments shows that Ni-DGS is the essential component causing the exchange. (A) Example cases of images for each case of lipid and peptide exchange. First raw is an example from the sample of 5 % Ni-DGS with LATpept, second from the 5 % Ni-DGS no peptides, and the third from 0 % Ni-DGS. Differential interference contras images are independent of fluorescence signal allowing us to unambiguously observe all vesicles regardless of the states. (B) Quantitative ratio of vesicles exchanged lipids and peptides at different SLB compositions. 5 % Ni-DG with LAT peptide bound, 5 % Ni-DGS without the peptides bound, and no Ni-DGS included at all. (C) Quantitative ratio of vesicles exchanged lipids and peptides at different GUV compositions. 5 % PS (5 % DOPS, 30 % DOPE, 65 % DOPC) and higher 30 % PS (30 % DOPS, 30 % DOPE, 40 % DOPC) tested. ($N = 18$ for B and $N = 19$ for C images from two independently prepared lipid bilayers, error bars represents standard errors) (D) Example images of adherence at different buffer conditions. Wide-field fluorescence images by TR-DHPE in GUVs collected right at the focal point of SLB where two bilayers meet. When no interaction, as shown in glucose buffer (300 mM Glucose, 20 mM Hepes, pH 7.0), GUVs are mostly off focus due to lack of interaction. In Saline buffer condition (150 mM NaCl, 20 mM Hepes pH 7.4) mild adhesion between bilayers start to develop. Scale bars are 10 μm.

signal unambiguously indicate exchange of lipids or peptides with SLB. What to count in fluorescence channels was usually also unambiguous for spontaneous exchange samples because such exchange usually happened as a clear stochastic yes or no fashion. It means the outcome of exchange was not a continuum of intensities in fluorescence signal, rather strong enough signal to be identified or none for each vesicle.

3. Results and discussion

3.1. Small membrane bound peptides spontaneously transfer between supported lipid bilayer and giant unilamellar vesicles

Fig. 1A shows a schematic of the peptide exchange experiment between SLB and GUV. Our original goal was to create a synthetic system capable of trafficking membrane peptides between SLB and GUV catalyzed by known fusogenic conditions such as cationic shock, glass nanoparticles, and freeze thawing [20–25,40]. During the investigation, we unexpectedly learned that spontaneous peptide transfer between SLB and GUV occurs reproducibly under the condition of neutral physiological saline buffer (20 mM Hepes, 150 mM NaCl, pH 7.4) that we decided to study in details.

To test the peptide transfer, SLB was formed on piranha-etched coverglass (5 % Ni-DGS, 30 % DOPE, 54.9 % DOPC, and 0.1 % DiD by mol%). Ni-DGS was used to covalently anchor fluorescently labeled small peptides (LAT peptide derived from the mammalian T-cell signaling protein [33,41]) to the SLB using his-tags. GUVs were

introduced by gentle pipetting and the state of peptide exchange was monitored by CLSM images. SLB lipids, GUV lipids, and peptides were each labeled with different wavelengths of fluorescence reporters in order to monitor the change of lipid membrane morphology and exchange of molecules by fluorescence image analysis. Multiple images were collected after 30 min of interaction between SLB and GUV, and images were analyzed for quantification.

Representative images for the case of peptide exchange is shown in Fig. 1B. Green fluorescence from LAT-OG488 is clearly observed in the GUV suggesting the transfer of the peptides. We quantified the degree of exchange by calculating the number of pixels where signals from different channels colocalize in the image with peptide fluorescence divided by the total number of pixels with lipid fluorescence. Fig. 1C shows the quantitative comparison of peptides on the membranes between the negative control (which only included DiD lipid fluorescence reporter) and the peptide exchanged vesicles. The ratio below 0.01 of the control sample represents the noise level. As shown in the quantification, exchange of peptide is clear although not all lipids membranes ended up taking up the peptides from the SLB. 0.04 of ratio might seem relatively low, but the case of peptide exchange was very clearly observable by fluorescence, evenly distributed in different regions of the samples, and reproducible. It shows that certain ratio of GUV-SLB contact interactions led to spontaneous exchange of membrane bound peptides under the physiological ionic strength and pH, and not all contact interactions led to the successful exchange of peptides.

3.2. Peptide exchange between membranes involve lipid exchange

We hypothesized that membrane peptide transfer occurs as a result of natural lipids exchange between SLB and GUV. The lipid intensities of vesicles that showed peptide transfer were analyzed to monitor the degree of lipid exchange using the pixel number analysis similar to Fig. 1. Number of pixels with TR-DHPE (lipids originally in SLB) over number of pixels with DiD (lipids originally in GUV) was quantified only for pixels with LAT-OG488 as a result of peptide exchange. The quantitation indeed showed that vesicles that took up the peptides did exchange lipids evidenced by 0.70 of the TR-DHPE/DiD ratio (Fig. 2A). It means most lipid membranes that took up peptides had lipid fluorescence from reporters that were originally in GUVs and in SLB both. Such process of lipid exchange often involved observable diffusion of reporter fluorescence, originally in GUV, across the SLB surface showing that the process does involve thermal diffusion (Supplementary S2). Also notable is that DiD fluorescence pixel counting usually did not reach zero after the exchange. It means a certain amount of DiD reporters, originally in GUVs still remained after the interaction. This observation supports the idea that the exchange occurs by hemi-fusion involving the fusion of only one leaflet instead of the full fusion of both leaflets which would inevitably lead to depletion of DiD fluorescence in GUV after the lipid exchange [21,24,40,42–44]. This is because the amount of lipids in each vesicle is limited compared to the amount of lipids in SLB which is a fluidic bilayer spanning the entire cover glass. If only one of the two leaflet was to hemi-fuse, fluorescence reporters in the unfused leaflet of the vesicles would still remain. Overall, the analysis suggests that the peptide transfer involves lipid transfer between two fluidic membranes and the observed peptide exchange is not an event that is only specific to the peptides.

3.3. Time lapse images show that the peptides are transferred by occasional hemi-fusion bridge formation mechanism

To better monitor the dynamic process of the peptide and lipid exchange, we used different sets of fluorescent reporters and took time lapse movies at the contact site between the GUV and SLB using wide field fluorescence microscopy. Fig. 3 shows example time-lapse movies at the contact site and z-section images after the exchange. Fig. 3AB images were taken by fluoresce reporters of TR-DHPE in SLB, A647 on peptides, and Fig. 3C images were taken by fluorescence reporters of A647 on peptides only. GUVs were colorless initially with no fluorescence reporters. Making GUVs colorless initially made the dynamics of lipids and peptides exchange more clearly visible as what used to be invisible would become visible only after taking up the fluorescence from SLB. Fig. 3A shows progress of most typical modes of peptide exchange, Fig. 3B shows relatively rare case of fragmented progress, and Fig. 3C shows an example images of the sample after the peptide exchange happened. Before GUVs contacted SLB, peptide fluorescence was evenly distributed showing homogeneous distribution of peptides on the SLB. As shown in Fig. 3A, once GUVs landed to make contact, dark peptide fluorescence became visible suggesting peptides were being excluded at the contact site. Such exclusion was not as pronounced in the lipid channel suggesting that this was physical exclusion of peptides at the contact site due to proximity of two lipid membranes. This dark spot was followed by intermittent peptide fluorescence among the dark spot, and soon the colorless GUVs took up the fluorescence of both lipids and peptides simultaneously suggesting exchange of lipids and peptides. The GUVs that used to be invisible due to lack of fluorescence reporters became clearly visible at this point.

We hypothesize this is by forming hemi-fusion lipid bridges between SLB and GUVs as shown in the schematic of Fig. 1A. We saw multiple inhomogeneous fluorescence fluctuations at the contact sites before fluidity was established between GUV and SLB, so we assume majority of the area at the contact sites were involved in hemi-fusion. It is unlikely though each GUV was forming a single hemi-fusion diaphragm spanning the entire area of the entire site with SLB because such single diaphragm formation would involve peptide diffusion only at the very edge of the hemi-fusion site. More likely mechanism is that multiple intermittent hemi-fusion bridges were formed as evidenced by visible diffusion of peptides at the contact site. Our time lapse movies were taken every 30 s, and lipid/peptide exchange typically occurred within a time frame once started, this timescale is close to the natural diffusion rate of the lipids and proteins in SLB [45]. In no case did we observe GUVs collapsing to become a continuous bilayer with the original SLB nor had the SLB budded out to create new vesicles. We did see however, some rare cases where the landed GUVs fragmented into smaller vesicles before the exchange happened (Fig. 3B). We assume this is a large GUV being fragmented due to GUV-SLB interaction followed by smaller GUVs exchanging lipids and peptides by forming hemi-fusion bridges. Many vesicles remained in position suggesting such hemi-fused structure may stay, but there were also some vesicles that were free to diffuse in solution indicating reversing the hemi-fusion state of an individual GUV to leave the contact site is possible resembling the “kiss an run” mechanism, temporary fusion of a vesicle at the contact site followed by fission, in the trafficking of neurotransmitter and endocytosis [46].

Fig. 3C clearly summarizes the observation. Contact sites excluded peptides making them clearly visible, but only some of the contacts led to successful exchange of peptides making the GUVs visible by the peptide fluorescence. When such an exchange took place, the outcome was clearly visible. FRAP images showing fluidity of SLB-GUV hemi-fused site can be found in Supplementary S3. GUVs mostly retained the morphologies as vesicles sitting on SLB instead of being entirely fused with SLB. At this point, further major change was seldom observed. Example fluorescence intensity kinetic trace analysis with more time lapse examples is also available in Supplementary S4 where it is clear that peptide exchange and lipid exchange happen simultaneously in the time scale of minutes.

3.4. Larger protein cargos do not transfer between SLB and GUV

Hinted by the lipid exchange resulting in spontaneous transfer of small peptides between SLB and GUV, we tested if larger peripheral proteins comparable to the size of a typical protein cargo of tens of kD with addition of a few small protein modifiers on the lipid membranes may be transferred the same way [47]. We performed a similar

experiment with SUMO3-GFP cargo instead of small peptides anchored to the SLB. SUMO protein is a small protein modifier that is often attached to a target protein to affect their metabolism and function and GFP is a fluorescent reporter commonly used in cellular imaging [36]. Overall, this cargo is 77 kD (27kD EGFP + 50kD SUMO3 with tags) which is much greater in size compared to the small LAT peptide (4kD). They were anchored to the lipid membrane using an identical chemistry of his-tag Ni binding, and were free to diffuse with lipids in the membranes.

As shown in Fig. 4, unlike small peptides, these larger membrane cargos failed to spontaneously transfer between SLB and GUV at least not to the level of clearly quantifiable amount. Visual observation showed no apparent protein bound vesicles emerged as a result of the interaction. We interpret this as a result of the bulkiness of protein size preventing larger proteins to diffuse across the lipid bridge stalks between SLB and GUVs. The geometry of bridges between SLB and GUV are speculated to be challenging for bulky membrane proteins to freely diffuse due to highly curved shape that is necessary to achieve intermittent lipid stalks between proximal bilayers.

3.5. Facilitating further lipid exchange by cationic shock does not enhance the efficiency of the peptide exchange

To further test the hypothesis of small peptides being transferred by passive diffusion along with lipids, we used a fusogenic condition of highly charged cationic shock by trivalent La^{3+}. By the cationic shock, we catalyzed the lipid exchange between SLB and GUV to monitor if the peptide exchange was enhanced by the increased amount of lipid exchange. It was the choice of fusogenic condition because La^{3+} is known to induce fusion between lipid bilayers [20], and a previous report showed divalent cation Ca^{2+} could catalyze lipid exchange between SLB and GUV [40].

As quantified in Fig. 5A cationic shock did increase the amount of lipid exchange between SLB and GUVs as evidenced by the increased TR/DiD pixel ratio to 0.14. We could occasionally see induced fusion among GUVs as well at this condition (Supplementary S2). However, against the assumption of catalyzing lipid exchange inducing more peptide exchange, the amount of peptide exchange remained unchanged before and after the cationic shock (Fig. 5B). Related to the larger protein exchange experiments, this result suggests that while lipid exchange is a prerequisite for the transfer of membrane-bound peptides, lipid exchange alone is an insufficient condition for peptide exchange. In this case, cationic shock catalyzed the lipid exchange between SLB and GUV, but could not further catalyze the exchange of peripheral peptides. Experiments performed by Ca^{2+} as a fusogenic condition showed a similar result suggesting that this is the case for both multivalent cations. (Supplementary S5).

3.6. Fluidic state of the lipid bilayers is necessary condition for peptide and lipid exchange

After discovering the spontaneous transfer of peptides between SLB and GUVs, we performed systematic investigation of lipid composition dependence experiments to obtain better insight regarding the molecular mechanism of such exchange. We hypothesized fluidic bilayer is necessary as the peptide transfer always involved the exchange of lipids between two bilayers. This was indeed the case. We replaced the fluidic lipids of the original SLB into immobile 1,2-dipalmitoyl-sn-glycero-3-phosphocholine (DPPC), a high melting temperature lipids creating immobile gel phase bilayer [48] at room temperature. (5 % Ni-DGS, 94.9 % DPPC, 0.1 % OG488-DHPE) The SLB was still functionalized with LAT-A647 peptides similar to experiments in Figs. 2 and 3. Fluidic GUVs (5 % DOPS, 30 % DOPE, 64.9 % DOPC, 0.1 % TR-DHPE) were allowed to interact with SLB like previous experiments in Figs. 2 and 3. As shown in Fig. 6A, there was no detectable exchange of lipids between SLB and GUV when immobile SLB was used. Exchange of lipids would make fluorescent reporter in SLB to appear in GUV fluorescence that we never saw when existence of GUV was still obvious as evidenced by matching DIC images. Fig. 6B is a quantification graphs comparing fluidic and immobile case, and basically there was no interaction of lipid exchange at all when SLB was immobile which makes sense considering the fact that thermal diffusion of lipids across the bilayers will be necessary for the lipid exchange to happen. It shows that the fluidic lipids is what mediate the peptide exchange, and it is a necessary condition for the exchange to happen.

3.7. Compositional study shows that the peptide exchange is dependent on the Ni-DGS functional lipids

As the peptide transfer was the event of interest, we next sought dependence of the lipid and peptide exchanges at varying conditions of SLB functionalization. Specifically, we tested and quantified the degree of lipid and peptide exchange when there was no peptide engineered on SLB, and when there was no functionalization lipid Ni-DGS at all compared to the normal cases of spontaneous peptide exchange. This way, potential importance of each component could be revealed. We did this as two-color wide field imaging to minimize any crosstalk between color channels and unambiguously determine the exchanges aided by DIC imaging. SLB lipids were labeled by OG488-DHPE and the LAT peptide by Alexa647. GUVs that are fluorescently invisible were detected by DIC imaging. The data for this series of experiments were analyzed by counting analysis as described in the Methods section.

Fig. 7A shows example cases of how the vesicle images looked like for different outcome of states. Only when lipids and peptides were exchanged between SLB and GUVs, the vesicle appeared in all three channels of images. The experiments proved that the Ni-DGS lipid is the key component behind the spontaneous peptide transfer as shown in Fig. 7B. When Ni-DGS was exposed barely without binding to LAT, it actually even enhanced the amount of lipid exchange between SLB and GUV suggesting that Ni-DGS facilitates the spontaneous exchange process. When Ni-DGS was removed from SLB, any interaction between SLB and GUV was minimized significantly below 1 % of the vesicles making it much harder to find any case of interactions between SLB and GUVs.

Since Ni-DGS bears a positive charge, we hypothesized that the negative charge of the DOPS in GUV may play an important role in the interaction. To test this, higher DOPS mol % GUVs were tested under otherwise identical condition. If DOPS is a catalyst, this would increase the degree of interaction. However, as shown in Fig. 7C, increasing DOPS mol% did not increase the degree of lipids and peptides exchange between SLB and GUV suggesting that having more negative charge on vesicles do not necessarily enhance the likelihood of the peptide transfer.

We also varied the ionic strength of the buffer used to observe its effect. When we observed interaction between SLB and GUVs at the very interface using fluorescently labeled TR-DHPE lipids in GUV using a glucose buffer, where no ions were added, we observed almost no interaction as evidenced by all GUVs being clearly off focus at the interface (Fig. 7D) Under the saline buffer condition we used in our experiments, mild adhesion developed given enough time evidenced by fluoresce signal of flattened membrane of the GUVs. In all cases, inside the vesicles were sucrose solution of iso-osmotic concentration. It suggests that the saline buffer environment (existence of ions) promotes adhesion interaction between SLB and GUV, presumably affecting electrostatic interactions among participating molecules [49], although it cannot be said that it is necessarily responsible for the following fusion and peptide transfer.

While the data suggest Ni-DGS plays a vital role in the process, it is worth pointing out that there is no experimental evidence to speculate the specific sequence of the peptide used had any essential role in the process. The LAT peptide, as the sequence shown in the Methods section, was a largely flexible peptide with glycine linker between essential peptide sequences [33] responsible for binding of the downstream

signaling proteins in the T-Cell signaling process [50–53]. Overall, there were two net positive residues and three net negative residues with two phospho-tyrosines in the sequence. It means, overall, each peptide was net $-1 \sim -3$ charged at neutral pH considering the fact that phosphate group may be hydrolyzed spontaneously. It is unlikely that the peptides could establish any attractive electrostatic interaction with the GUVs which contained net negatively charged PS lipids, nor the sequence is particularly hydrophobic to directly insert itself into the lipid bilayer [54].

3.8. Current model of the peptide transfer

Our work reports a case of synthetic lipid membrane system trafficking membrane peptides spontaneously under the neutral pH 7.4 and physiological ionic strength of 150 mM NaCl condition. The work is part of our group's effort to construct a minimal synthetic membrane system to perform an efficient trafficking of membrane bound proteins. Our result serves an example platform where membrane bound peptide can be transferred between SLB and GUV, and also shed hint on the mechanism of membrane protein transfer between relatively large (>1 μm^2) lipid bilayers.

Our hypothetical model for the peptide transfer is that when SLB and GUVs form contact sites, occasional lipid hemi-fusion bridges form. Lipids can thermally diffuse across the bridge, and membrane anchored protein cargos can cross the bridge when their sizes are small enough to diffuse through the highly curved lipid bridges. This is evidenced by the experiment where larger SUMO3-GFP cargos could not be transferred while smaller LAT peptides could be transferred between the membranes. Catalyzing the lipid exchange by cationic shock could not further enhance the chance of peptide transfer and it suggests that catatonically catalyzed lipid exchange occurs by a different mechanism that does not provide a chance for small peripheral peptides to transfer. Saline buffer condition is necessary promoting initial adhesion contact between bilayers when vesicles come close proximity to the SLB, and Ni-DGS lipids are responsible catalyzing the hemi-fusion bridge formation between the bilayers. Throughout the process, fluidic state of the bilayers is strictly required for the exchange to happen suggesting the process involve thermal diffusion of molecules across the bilayers.

As to how Ni-DGS promotes such exchange process, and why it is not promoting it to the level where majority of vesicles experience such exchange is unclear. At this point, it is evident that the electrostatic interaction plays the key role in the process. Multivalent cations are known to strongly interact with lipid head-groups and cause fusion, lipid exchange, clustering of lipids, and deformation [20,40,55–57]. Ni^{2+} especially in its chelated form inducing similar effect has been unknown, but our finding suggests that it may be able to catalyze the hemi-fusion between bilayers presumably by a similar interaction with other multivalent cations. Future studies should include detailed investigation of the Ni-DGS dependency of the phenomena to fully decipher the mechanism behind the transfer. The future effort should also aim to find conditions where such transfer can be catalyzed to happen a lot more efficiently and frequently.

Some alternative explanations of the observed exchange that deserve commenting include lipid oxidation and mechanical stress. Lipids are known to be vulnerable to oxidation process which can change the bilayer properties [32,58]. Lipid oxidation during the GUV incubation is an unlikely contributor to the phenomena as we did not see difference when we shortened the GUV incubation time to minimize the chance of oxidation during the incubation process. (Supplementary S6) Spontaneous exchange occurred even at the regions where no fluorescence illumination was applied, so it is also unlikely any photo oxidation processes were involved. Osmotic imbalance across the membrane is known to impose mechanical stress to the lipid membranes that could lead to reorganization of lateral structure [59], and membrane deformation [60]. The saline condition we used was supposed to be isoosmotic to sucrose inside the vesicle by design, but a subtle osmotic imbalance may still have imposed mechanical stress to the vesicles. We believe this is highly unlikely that the osmotic imbalance is a sufficient condition for the lipids and peptides exchange though, because such imbalance would be universal across all samples tested that we did not always see the exchange happening.

Our work suggests an experimental platform to establish peptide exchange between SLB and GUVs, and provides a hypothetical model of peptide transfer, but caution should be taken interpreting the results. Firstly, even though the observed spontaneous exchange was reproducible and clearly observable in all our experiments with various combinations of dyes used, not every GUV showed such exchange after contacting with SLBs. We tested a prolonged incubation assuming this was merely due to a very slow kinetic process, but we could not find evidence that longer incubation led to successful peptide transfer of every vesicle. (Supplementary S7) It may suggest that certain vesicles are in the 'right' condition to spontaneously react with SLB which is dependent on unknown parameters such as membrane tension, or exact lipid composition. Most outcome was clear cut stochastic as exchanged or none instead of continuum of signals. Secondly, Ni-DGS was used as a necessary component to anchor peptides and proteins by his-tag chelation, and it also turned out to be the essential component promoting the process. We speculate Ni-chelation chemistry might be influenced by the cationic shock condition affecting the final outcome of the cationic shock experiments. Thirdly, our schematic figures show the final stages of the exchange as freed vesicles from the hemi-fusion, but most images analyzed represent analysis vesicles analyzed as still adhered to the SLB. We did occasionally see detached vesicles floating around in the samples as mentioned in the discussion, but caution should be used because most vesicles analyzed remained sitting on SLB.

4. Conclusion

We report a case of synthetic lipid membrane platform capable of trafficking small membrane bound peptides from SLB to GUVs. A series of experiments support the model that the transfer occurs by formation of hemi-fused lipid stalks between GUV and SLB that are highly curved limiting diffusion of larger protein cargos. It suggests peripheral peptides may transfer between the membranes by occasional hemi-fusion interaction and the transfer is limited by the geometry of the lipid bridge which is hypothesized to be highly curved. Our composition dependent studies show that the bilayer adhesion is promoted by the ionic buffer condition, and the transfer process is catalyzed by the Ni-DGS lipids. Electrostatic interaction must play an important role in the process considering the key conditions. Our model provides an insight for a simple mechanism of lipid bilayers to interact at a neutral saline buffer condition to transfer membrane proteins spontaneously and serves an example of synthetic system capable of transferring small peptides between two lipid bilayers with a relatively large contact area (> 1 μm^2).

Potential future work includes further exploring the conditions of buffers and lipid compositions affecting the exchange with the goal of deciphering the detailed molecular mechanism, and single molecule tracking study to monitor the movement of peptide molecules at a higher spatial and temporal resolution to monitor the movement of peptide molecules diffusing across the hemi-fused stalks. Eventually, discovering conditions where larger protein cargos can be transferred is expected to provide us a useful functional platform of vesicular trafficking that is compatible with dynamic high-resolution imaging by optical microscopy.

Abbreviations

A647	Alexa fluor 647
CLSM	Confocal laser scanning microscope
DiD	1,1′-dioctadecyl-3,3,3′,3′-tetramethylindodicarbocyanine
DOPC	1,2-Dioleoyl-sn-glycero-3-phosphocholine

DOPE	1,2-dioleoyl-sn-glycero-3-phosphoethanolamine
DOPS	1,2-dioleoyl-sn-glycero-3-phospho-L-serine
DPPC	1,2-dipalmitoyl-sn-glycero-3-phosphocholine
FRAP	Fluorescence bleaching after photobleaching
GFP	Green fluorescence protein
GUV	Giant unilamellar vesicle
LAT	Linker for activation of T-cell
Ni-DGS	Nickel bound 1,2-Dioleoyl-sn-glycero-3-[(N-(5-amino-1-carboxypentyl)iminodiacetic acid)succinyl]
OG488	Oregon green 488
SLB	Supported lipid bilayer
SUMO	Small Ubiquitin-like modifier
TR-DHPE	Texas Red-1,2-Dihexadecanoyl-sn-Glycero-3-Phosphoethanolamine

Funding

The study was supported by the startup fund from the College of Science and Mathematics (CSAM), Montclair State University. The study was also supported by the National Science Foundation (NSF) Garden State-Louis Stokes Alliance for Minority Participation (GS-LSAMP) scholar award program (NSF award HRD-1909824). Emanuela Efodili gratefully acknowledges receiving a Post-Bac Research Experience for LSAMP Students (PRELS) stipend from the NSF through the GS-LSAMP. The study was also supported by the separately budgeted research, fiscal year 2023 (FY23 SBR), CSAM summer research program, CSAM research program, Montclair State University. Computational support was provided by Oracle for research grant (CPG-2695313).

Declaration of competing interest

The authors declare that they have no known competing financial interests or personal relationships that could have appeared to influence the work reported in this paper.

Data availability

Data will be made available on request.

Acknowledgements

The authors would like to thank Dr. Laying Wu of the Microscopy and microanalysis research laboratory at Montclair state university for the microscope training and facility maintenance.

Appendix A. Supplementary data

Supplementary data to this article can be found online at https://doi.org/10.1016/j.bbamem.2023.184256.

References

[1] J. Schöneberg, I.-H. Lee, J.H. Iwasa, J.H. Hurley, Reverse-topology membrane scission by the ESCRT proteins, Nat. Rev. Mol. Cell Biol. 18 (2017) 5–17.
[2] M. Kaksonen, A. Roux, Mechanisms of clathrin-mediated endocytosis, Nat. Rev. Mol. Cell Biol. 19 (2018) 313–326.
[3] Y. Guo, D.W. Sirkis, R. Schekman, Protein sorting at the trans-Golgi network, Annu. Rev. Cell Dev. Biol. 30 (2014) 169–206.
[4] L.V. Chernomordik, M.M. Kozlov, Membrane hemifusion: crossing a chasm in two leaps, Cell 123 (2005) 375–382.
[5] T.H. Söllner, Intracellular and viral membrane fusion: a uniting mechanism, Curr. Opin. Cell Biol. 16 (2004) 429–435.
[6] A. García-Cazorla, A. Oyarzábal, J.-M. Saudubray, D. Martinelli, C. Dionisi-Vici, Genetic disorders of cellular trafficking, Trends Genet. 38 (2022) 724–751.
[7] P.K. Singh, M.M.K. Muqit, Parkinson's: a disease of aberrant vesicle trafficking, Annu. Rev. Cell Dev. Biol. 36 (2020) 237–264.
[8] I.-H. Lee, H. Kai, L.-A. Carlson, J.T. Groves, J.H. Hurley, Negative membrane curvature catalyzes nucleation of endosomal sorting complex required for transport (ESCRT)-III assembly, Proc. Natl. Acad. Sci. 112 (2015) 15892–15897.
[9] A. Roux, G. Cappello, J. Cartaud, J. Prost, B. Goud, P. Bassereau, A minimal system allowing tubulation with molecular motors pulling on giant liposomes, Proc. Natl. Acad. Sci. 99 (2002) 5394.
[10] J. Schöneberg, M.R. Pavlin, S. Yan, M. Righini, I.-H. Lee, L.-A. Carlson, A. H. Bahrami, D.H. Goldman, X. Ren, G. Hummer, C. Bustamante, J.H. Hurley, ATP-dependent force generation and membrane scission by ESCRT-III and Vps4, Science 362 (2018) 1423.
[11] Y. Lyu, R. Peng, H. Liu, H. Kuai, L. Mo, D. Han, J. Li, W. Tan, Protocells programmed through artificial reaction networks, Chem. Sci. 11 (2020) 631–642.
[12] M. Imai, Y. Sakuma, M. Kurisu, P. Walde, From vesicles toward protocells and minimal cells, Soft Matter 18 (2022) 4823–4849.
[13] B.S. Pattni, V.V. Chupin, V.P. Torchilin, New developments in liposomal drug delivery, Chem. Rev. 115 (2015) 10938–10966.
[14] A. Bunker, A. Magarkar, T. Viitala, Rational design of liposomal drug delivery systems, a review: combined experimental and computational studies of lipid membranes, liposomes and their PEGylation, Biochim. Biophys. Acta (BBA) Biomembranes 1858 (2016) 2334–2352.
[15] M. Mettlen, P.-H. Chen, S. Srinivasan, G. Danuser, S.L. Schmid, Regulation of clathrin-mediated endocytosis, Annu. Rev. Biochem. 87 (2018) 871–896.
[16] A.J. Jimenez, P. Maiuri, J. Lafaurie-Janvore, S. Divoux, M. Piel, F. Perez, ESCRT machinery is required for plasma membrane repair, Science 343 (2014) 1247136.
[17] E.B. Frankel, R. Shankar, J.J. Moresco, J.R. Yates, N. Volkmann, A. Audhya, Ist1 regulates ESCRT-III assembly and function during multivesicular endosome biogenesis in Caenorhabditis elegans embryos, Nat. Commun. 8 (2017) 1439.
[18] J. Köfinger, Michael J. Ragusa, I.-H. Lee, G. Hummer, James H. Hurley, Solution structure of the Atg1 complex: implications for the architecture of the phagophore assembly site, Structure 23 (2015) 809–818.
[19] P.U. Ratnayake, K. Sackett, M.J. Nethercott, D.P., Weliky, pH-dependent vesicle fusion induced by the ectodomain of the human immunodeficiency virus membrane fusion protein gp41: two kinetically distinct processes and fully-membrane-associated gp41 with predominant β sheet fusion peptide conformation, Biochim. Biophys. Acta (BBA) Biomembranes 1848 (2015) 289–298.
[20] T. Tanaka, M. Yamazaki, Membrane fusion of giant unilamellar vesicles of neutral phospholipid membranes induced by La3+, Langmuir 20 (2004) 5160–5164.
[21] J. Nikolaus, M. Stöckl, D. Langosch, R. Volkmer, A. Herrmann, Direct visualization of large and protein-free hemifusion diaphragms, Biophys. J. 98 (2010) 1192–1199.
[22] T. Litschel, K.A. Ganzinger, T. Movinkel, M. Heymann, T. Robinson, H. Mutschler, P. Schwille, Freeze-thaw cycles induce content exchange between cell-sized lipid vesicles, New J. Phys. 20 (2018), 055008.
[23] Y.T. Sato, K. Umezaki, S. Sawada, S.-A. Mukai, Y. Sasaki, N. Harada, H. Shiku, K. Akiyoshi, Engineering hybrid exosomes by membrane fusion with liposomes, Sci. Rep. 6 (2016) 21933.
[24] M. Arribas Perez, P.A. Beales, Biomimetic curvature and tension-driven membrane fusion induced by silica nanoparticles, Langmuir 37 (2021) 13917–13931.
[25] M.A. Tahir, Z.P. Guven, L.R. Arriaga, B. Tinao, Y.-S.S. Yang, A. Bekdemir, J. T. Martin, A.N. Bhanji, D. Irvine, F. Stellacci, A. Alexander-Katz, Calcium-triggered fusion of lipid membranes is enabled by amphiphilic nanoparticles, Proc. Natl. Acad. Sci. 117 (2020) 18470–18476.
[26] N. Kahya, E.-I. Pécheur, W.P. de Boeij, D.A. Wiersma, D. Hoekstra, Reconstitution of membrane proteins into giant unilamellar vesicles via peptide-induced fusion, Biophys. J. 81 (2001) 1464–1474.
[27] P. Wadhwani, J. Reichert, J. Bürck, A.S. Ulrich, Antimicrobial and cell-penetrating peptides induce lipid vesicle fusion by folding and aggregation, Eur. Biophys. J. 41 (2012) 177–187.
[28] R.J. Rawle, B. van Lengerich, M. Chung, P.M. Bendix, S.G. Boxer, Vesicle fusion observed by content transfer across a tethered lipid bilayer, Biophys. J. 101 (2011) L37–L39.
[29] Y. Uwaguchi, K. Fujiwara, N. Doi, Switching ON of transcription-translation system using GUV fusion by co-supplementation of calcium with long-chain polyethylene glycol, ChemBioChem 22 (2021) 2319–2324.
[30] N. Marušič, L. Otrin, J. Rauchhaus, Z. Zhao, F.L. Kyrilis, F. Hamdi, P.L. Kastritis, R. Dimova, I. Ivanov, K. Sundmacher, Increased efficiency of charge-mediated fusion in polymer/lipid hybrid membranes, Proc. Natl. Acad. Sci. 119 (2022), e2122468119.
[31] J. Ureña, A. Knight, I.-H. Lee, Membrane cargo density-dependent interaction between protein and lipid domains on the giant unilamellar vesicles, Langmuir 38 (2022) 4702–4712.
[32] N.F. Morales-Penningston, J. Wu, E.R. Farkas, S.L. Goh, T.M. Konyakhina, J. Y. Zheng, W.W. Webb, G.W. Feigenson, GUV preparation and imaging: minimizing artifacts, Biochim. Biophys. Acta (BBA) Biomembranes 1798 (2010) 1324–1332.
[33] I.-H. Lee, M.Y. Imanaka, E.H. Modahl, A.P. Torres-Ocampo, Lipid raft phase modulation by membrane-anchored proteins with inherent phase separation properties, ACS Omega 4 (2019) 6551–6559.
[34] A.V. Botelho, N.J. Gibson, R.L. Thurmond, Y. Wang, M.F. Brown, Conformational energetics of rhodopsin modulated by nonlamellar-forming lipids, Biochemistry 41 (2002) 6354–6368.
[35] W.C. Lin, C.H. Yu, S. Triffo, J.T. Groves, Supported membrane formation, characterization, functionalization, and patterning for application in biological science and technology, Curr. Protoc. Chem. Biol. 2 (2010) 235–269.
[36] S.F. Banani, A.M. Rice, W.B. Peeples, Y. Lin, S. Jain, R. Parker, M.K. Rosen, Compositional control of phase-separated cellular bodies, Cell 166 (2016) 651–663.
[37] J.A. Nye, J.T. Groves, Kinetic control of histidine-tagged protein surface density on supported lipid bilayers, Langmuir 24 (2008) 4145–4149.

[38] C.I. McPhee, G. Zoriniants, W. Langbein, P. Borri, Measuring the lamellarity of giant lipid vesicles with differential interference contrast microscopy, Biophys. J. 105 (2013) 1414–1420.
[39] I.-H. Lee, S. Passaro, S. Ozturk, J. Ureña, W. Wang, Intelligent fluorescence image analysis of giant unilamellar vesicles using convolutional neural network, BMC Bioinformatics 23 (2022) 48.
[40] T.A. Enoki, G.W. Feigenson, Asymmetric bilayers by hemifusion: method and leaflet behaviors, Biophys. J. 117 (2019) 1037–1050.
[41] S. Sun, T. GrandPre, D.T. Limmer, J.T. Groves, Kinetic frustration by limited bond availability controls the LAT protein condensation phase transition on membranes, Sci. Adv., 8 eabo5295.
[42] T.-T. Kliesch, J. Dietz, L. Turco, P. Halder, E. Polo, M. Tarantola, R. Jahn, A. Janshoff, Membrane tension increases fusion efficiency of model membranes in the presence of SNAREs, Sci. Rep. 7 (2017) 12070.
[43] T.A. Enoki, J. Wu, F.A. Heberle, G.W. Feigenson, Investigation of the domain line tension in asymmetric vesicles prepared via hemifusion, Biochim. Biophys. Acta (BBA) Biomembranes 1863 (2021), 183586.
[44] P. Shendrik, G. Golani, R. Dharan, U.S. Schwarz, R. Sorkin, Membrane tension inhibits lipid mixing by increasing the hemifusion stalk energy, ACS Nano 17 (2023) 18942–18951.
[45] I.-H. Lee, S. Saha, A. Polley, H. Huang, S. Mayor, M. Rao, J.T. Groves, Live cell plasma membranes do not exhibit a miscibility phase transition over a wide range of temperatures, J. Phys. Chem. B. 119 (2015) 4450–4459.
[46] A.A. Alabi, R.W. Tsien, Perspectives on kiss-and-run: role in exocytosis, endocytosis, and neurotransmission, Annu. Rev. Physiol. 75 (2013) 393–422.
[47] K. Haglund, I. Dikic, Ubiquitylation and cell signaling, EMBO J. 24 (2005) 3353–3359.
[48] Y.-T. Ti, H.-C. Cheng, Y. Li, H.-L. Tu, Multiplexed patterning of hybrid lipid membrane and protein arrays for cell signaling study, Lab Chip 21 (2021) 2711–2720.
[49] J. Solon, P. Streicher, R. Richter, F. Brochard-Wyart, P. Bassereau, Vesicles surfing on a lipid bilayer: self-induced haptotactic motion, Proc. Natl. Acad. Sci. 103 (2006) 12382–12387.
[50] W.Y.C. Huang, S. Alvarez, Y. Kondo, Y.K. Lee, J.K. Chung, H.Y.M. Lam, K. H. Biswas, J. Kuriyan, J.T. Groves, A molecular assembly phase transition and kinetic proofreading modulate Ras activation by SOS, Science 363 (2019) 1098–1103.
[51] W.Y.C. Huang, Q. Yan, W.-C. Lin, J.K. Chung, S.D. Hansen, S.M. Christensen, H.-L. Tu, J. Kuriyan, J.T. Groves, Phosphotyrosine-mediated LAT assembly on membranes drives kinetic bifurcation in recruitment dynamics of the Ras activator SOS, Proc. Natl. Acad. Sci. 113 (2016) 8218–8223.
[52] X. Su, J.A. Ditlev, E. Hui, W. Xing, S. Banjade, J. Okrut, D.S. King, J. Taunton, M. K. Rosen, R.D. Vale, Phase separation of signaling molecules promotes T cell receptor signal transduction, Science 352 (2016) 595–599.
[53] H.-Y. Wang, S.H. Chan, S. Dey, I. Castello-Serrano, M.K. Rosen, J.A. Ditlev, K. R. Levental, I. Levental, Coupling of protein condensates to ordered lipid domains determines functional membrane organization, Sci. Adv. 9 (2023), eadf6205.
[54] J.P. Ulmschneider, J.C. Smith, S.H. White, M.B. Ulmschneider, In silico partitioning and transmembrane insertion of hydrophobic peptides under equilibrium conditions, J. Am. Chem. Soc. 133 (2011) 15487–15495.
[55] A. Melcrová, S. Pokorna, S. Pullanchery, M. Kohagen, P. Jurkiewicz, M. Hof, P. Jungwirth, P.S. Cremer, L. Cwiklik, The complex nature of calcium cation interactions with phospholipid bilayers, Sci. Rep. 6 (2016) 38035.
[56] M.F. Poyton, S. Pullanchery, S. Sun, T. Yang, P.S. Cremer, Zn2+ binds to phosphatidylserine and induces membrane blebbing, J. Am. Chem. Soc. 142 (2020) 18679–18686.
[57] C.F. Monson, X. Cong, A.D. Robison, H.P. Pace, C. Liu, M.F. Poyton, P.S. Cremer, Phosphatidylserine reversibly binds Cu2+ with extremely high affinity, J. Am. Chem. Soc. 134 (2012) 7773–7779.
[58] T.M. Tsubone, M.S. Baptista, R. Itri, Understanding membrane remodelling initiated by photosensitized lipid oxidation, Biophys. Chem. 254 (2019), 106263.
[59] K. Oglęcka, P. Rangamani, B. Liedberg, R.S. Kraut, A.N. Parikh, Oscillatory phase separation in giant lipid vesicles induced by transmembrane osmotic differentials, eLife 3 (2014), e03695.
[60] Y. Dreher, K. Jahnke, E. Bobkova, J.P. Spatz, K. Göpfrich, Division and regrowth of phase-separated giant unilamellar vesicles**, Angew. Chem. Int. Ed. 60 (2021) 10661–10669.